Negative-U defect: Interstitial boron in silicon

R. D. Harris,* J. L. Newton,† and G. D. Watkins
Department of Physics, Sherman Fairchild Laboratory, Lehigh University, Bethlehem, Pennsylvania 18015
(Received 13 June 1986; revised manuscript received 5 March 1987)

Novel optical deep-level-transient-spectroscopy (DLTS) studies are reported which reveal a new level (the single-donor level) of interstitial boron in silicon located at $E_c-(0.13\pm0.01)$ eV. Detailed studies of this level and the previously detected single-acceptor level at $E_c-(0.37\pm0.08)$ eV establish that these levels lie in negative-U ordering. A large Poole-Frenkel effect in the DLTS observed emission rate is apparent, and when properly accounted for provides a direct and unambiguous connection to the EPR-identified interstitial boron atom.

I. INTRODUCTION

A defect has negative-U properties[1] if it can trap two electrons with the second more strongly bound than the first. It is as if there were a net attraction between the two carriers (negative Hubbard correlation energy[2]). This possibility was first put forth by Anderson[3] and extended by Street and Mott[4] as a possible explanation for the observed properties of the chalcogenide glasses. These authors suggested that the energy gained by electron pairing plus a lattice relaxation[3,4] or configurational change[5] might overcome the Coulombic repulsion of the two electrons at the site. This would supply the effective net attraction needed to give a defect negative-U properties. Although this explanation is a reasonable one for the properties of the chalcogenide glasses, there has, however, as yet been no direct *microscopic* evidence to confirm this for these materials.

In the present paper, we demonstrate conclusively that interstitial boron in crystalline silicon has negative-U properties. When the results of this study were first presented,[6] they represented the first unambiguous identification of a defect with this property in any solid. Since then, an additional defect has also been identified to have this property—the lattice vacancy in silicon.[7] Convincing evidence of negative-U character has also been presented for defects in InP,[8] although the microscopic identity of the defects is lacking. Finally, recent optical studies in the chalcogenide glasses have been interpreted to confirm negative-U character for their dominant defects, giving $U=-1.0$ eV in a-As_2S_3 and $U=-0.7$ eV in As_2Se_3.[9]

Negative-U properties for defects in semiconductors are therefore now well established. In the present paper we present for the first time a detailed description of our experimental studies on interstitial boron.

Interstitial boron is one of the dominant defects produced in boron-doped crystalline silicon by electron irradiation (1–3 MeV) at cryogenic temperatures (4.2 K, 20.4 K).[10–12] It has been studied by both electron paramagnetic resonance (EPR) (Ref. 10) and deep-level transient spectroscopy (DLTS).[11,12] The first suggestion that it had negative-U properties was made by Watkins and Troxell[11,12] after a combined analysis of these EPR and DLTS results.

In the present study, this suggestion has been pursued in experiments which employ the addition of optical techniques to the normal DLTS experiment. A new electrical level is detected at $E_c-0.13$ eV, which we conclude is the single-donor level of interstitial boron. Detailed correlation of the properties of this level with those of a previously detected level at $E_c-0.37$ eV,[11,12] (previously located at $E_c-0.45$ eV, see Ref. 13) which we confirm is the single-acceptor level, unambiguously confirm the negative-U properties of the center. In addition, a large Poole-Frenkel effect in the DLTS observed emission rate from the $E(0.13)$ donor level is observed. When this is properly accounted for, a direct and unambiguous correlation to the EPR-identified interstitial boron atom is provided.

II. EXPERIMENTAL PROCEDURE

A. Deep-level transient spectroscopy (DLTS)

For studies in n-type material, p^+-n diodes were fabricated from partially counterdoped pulled silicon wafers that had been doped during growth with $\sim3\times10^{16}$ cm^{-3} phosphorus and $\sim1\times10^{16}$ cm^{-3} boron. [This is the same material used in the previous DLTS (Refs. 11 and 12) studies in n-type silicon.] The diodes were fabricated in a mesa configuration in order to allow optical access to the junction region from the side of the structure.

For studies in p-type material, two different structures were employed. n^+-p diodes and Schottky-barrier diodes (chromium contact) were fabricated on boron-doped ($\sim1.5\times10^{15}$ cm^{-3}) floating-zone silicon. The n^+-p diodes had a small metal contact placed over a larger diffused n^+ region so as to allow for optical access from the top of the structures. The Schottky-barrier diodes were fabricated in a mesa configuration to allow optical access to the junction from the side.

In all cases, following fabrication, the diodes were diced and mounted on TO-5 headers using a silver-laden con-

ductive epoxy, and contacted by ultrasonic bonding of 1 mil aluminum (1 at. % silicon) wires.

Interstitial boron was produced for study by *in situ* electron irradiation from a Van de Graaff accelerator, using an Air Products Heli-Tran cryostat to maintain sample temperatures near 4.2 K during irradiation. The n-type samples were irradiated with 1.0–1.5 MeV electrons and the p-type samples with 2.4-MeV electrons. In all cases, total fluences were in the range of $\sim 5\times 10^{15}$ to $\sim 1\times 10^{16}$ electrons/cm^2.

The samples were subsequently studied while mounted in the same cryostat using a deep-level capacitance transient spectrometer of the type described by Lang.[14] The spectrometer employed a capacitance bridge operating at 10 MHz with transient detection by means of a double boxcar signal averager.[15] Optical access to the sample was gained through a Pyrex window in the Heli-Tran. Two different optical sources were used: (1) A tungsten source with a room-temperature silicon filter, in conjunction with the Pyrex window, provided 0.3 eV $\leq h\nu \leq$ 1.1 eV photoionizing illumination to the sample. (2) A Strobotac, synchronized with the DLTS spectrometer, provided optical trap-filling pulses which could be substituted for the normal electrical trap-filling pulses.

B. Electron paramagnetic resonance (EPR)

For EPR study, a p-type, boron-doped ($\sim 1.5\times 10^{16}$ cm^{-3}) floating-zone sample was used. This sample had previously been made high resistivity by prolonged electron irradiation ($\sim 10^{18}$ electrons/cm^2) and room-temperature anneal. For the present study, the sample was reirradiated with 2.5-MeV electrons *in situ* at 20.4 K to produce interstitial boron for study. The sample was initially irradiated to a fluence of 6.3×10^{16} electrons/cm^2 where most of the studies were performed, and then extended with a second irradiation to 1.3×10^{17} electrons/cm^2 for additional study.

Most of the experimental techniques relevant to the EPR studies have been described previously.[16,17] EPR studies were performed at ~ 20 GHz and interstitial boron was observed in dispersion in the temperature range of 54–66 K by having the microwave cavity immersed in pumped liquid and solid nitrogen. Temperature was measured by monitoring the pressure above the nitrogen. The so-called Si-G28 spectrum, arising from the neutral charge state of interstitial boron,[10] was photogenerated by introducing light to the sample via a fused quartz light pipe from outside the cryostat.

III. DISCUSSION OF PREVIOUS EPR AND DLTS RESULTS

The original EPR studies[10] were interpreted to indicate that interstitial boron exists in three charged states, B_i^+, B_i^0, and B_i^-, giving rise to two electrical levels within the silicon band gap, a single-donor $(0/+)$ level and a single-acceptor $(-/0)$ level. The neutral charge state is paramagnetic and gives rise to the EPR spectrum which was denoted Si-G28. This spectrum was observed in both boron-doped p-type silicon and boron-counterdoped n-type silicon, following *in situ* electron irradiation at cryogenic temperatures. The spectrum had to be photogenerated with near-band-gap light in both types of material.

In p-type silicon, made high resistivity by prolonged irradiation, the neutral charge state was found to persist at 20.4 K even after the light was removed.[10] Its Si-G28 spectrum was observed to disappear, however, in ~ 15 min at 50 K. This loss was interpreted as thermally activated electron emission from the neutral charge state:

$$B_i^0 \rightarrow B_i^+ + e^- \ . \tag{1}$$

indicating an energy level for the donor state near $\sim E_c - 0.15$ eV.

Subsequent DLTS studies detected only a single level for interstitial boron located at $E_c - 0.37$ eV;[11–13] a level near $\sim E_c - 0.15$ eV was not observed. Watkins and Troxell proposed that this could be explained if interstitial boron were a negative-U defect, where the acceptor $(-/0)$ level at $E_c - 0.37$ eV lies below the donor $(0/+)$ level near $\sim E_c - 0.15$ eV.[11,12] These authors cited indirect DLTS evidence to support this model. They also pointed out that a natural consequence of this model is that the donor level would not be observed in a normal DLTS experiment.

A crucial test of the negative-U model is the direct electrical detection of the single-donor level. This direct detection is the subject of the present paper, but before describing those results, let us review why the donor level is not observable in a normal DLTS experiment. The difficulty that arises is in getting the defect into the appropriate charge state, i.e., the neutral charge state, for DLTS observation.

According to the model put forth by Watkins and Troxell,[11,12] both the donor level and the acceptor level lie in the upper half of the silicon band gap. Therefore, a majority-carrier trap-filling pulse in p-type silicon will not change the charge state; the positive charge state will be the stable charge state under both zero and reverse bias. A minority-carrier electrical pulse in p-type silicon (forward bias injection of electrons) could conceivably cause the defect to trap an electron, thus producing the neutral charge state. However, it is experimentally found that this does not happen. Apparently the relative electron and hole capture rates are not favorable for this process.

In n-type silicon (counterdoped with boron) a different problem arises; the defect captures electrons too easily. Before the trap-filling pulse is applied, when the sample is under reverse bias, interstitial boron prefers to be in the positive charge state, B_i^+. During the first trap-filling pulse, the B_i^+ ions will easily capture electrons

$$B_i^+ + e^- \rightarrow B_i^0 \ , \tag{2}$$

due to the Coulombic attraction for electron capture. This places the defects in the desired neutral charge state.

The problem that arises in n-type material is that some of these now neutral defects will inevitably also capture a second electron

$$B_i^0 + e^- \rightarrow B_i^- \ , \tag{3}$$

placing the defect in the negative charge state. Those de-

fects in the negative charge state cannot ionize ($E_i \sim 0.37$ eV) at the low temperature necessary to observe the emission from the neutral charge state ($E_i \sim 0.15$ eV). Therefore, the negatively charged defects are effectively removed from the experiment. No matter how short the trap-filling pulse, some of the defects will unavoidably accumulate in the negative charge state during each pulse. With the repetitive pulses required by DLTS, all of the centers will rapidly accumulate in the negative charge state, leaving none in the neutral charge state to observe.

The donor level of interstitial boron is, therefore, not observable in a normal DLTS experiment. The donor level would be observable if a modification to the normal DLTS experiment could be made that would either: (1) allow the defect to get to, and only to, the neutral charge state in p-type and/or n-type silicon, or (2) avoid the accumulation of centers in the negative charge state in n-type silicon. In this paper it will be shown that the addition of optical techniques to the DLTS experiment provides the necessary modification.

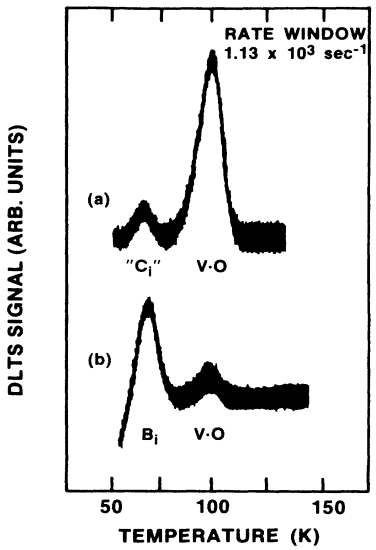

FIG. 1. Typical DLTS runs in n-type silicon after electron irradiation with (a) an electrical trap-filling pulse and (b) an optical trap-filling pulse. The B_i peak is visible only in (b).

IV. RESULTS

A. DLTS Results

From the previous EPR studies of interstitial boron,[10] it is known that the neutral charge state can be generated with near-band-gap light in both n-type and p-type silicon. This suggests that the use of an optical trap-filling pulse, instead of the normal electrical pulse, should generate the neutral charge state for DLTS study. The results of such an experiment are shown in Fig. 1, for an n-type sample, and in Fig. 2, for a p-type sample.

In Fig. 1, a typical set of DLTS scans through the temperature region where the donor level of interstitial boron is expected to appear is shown. In a normal DLTS scan [Fig. 1 curve (a)] with an electrical trap-filling pulse, two peaks are observed. These arise from a defect tentatively identified as interstitial carbon[15,18–20] [E(0.09), labeled "C_i" in the figure] and the vacancy-oxygen pair[15,16,18,21] [E(0.16), also called the A center and labeled V-O in the figure]. [The E(0.37) peak from interstitial boron is strong in this sample but appears at a much higher temperature than is shown in this figure.] When the electrical trap-filling pulse is replaced with an optical trap-filling pulse, Fig. 1 curve (b), the A center is still visible, although it is not as strong under these injection conditions. Another peak is visible at a temperature lower than the A center, approximately where the "interstitial carbon" peak appears. This new peak is at the approximate position that a peak arising from the single-donor level of interstitial boron is expected to appear. During the optical trap-filling pulse experiments the E(0.37) level is not observed, indicating that the B_i atom is not getting into the negative charge state.

The results shown in Fig. 1 already reveal that the new peak arises from a defect with very unusual electrical properties. The peak arises from an electron trap which is a majority-carrier trap in n-type silicon. However, it is not observed in a normal DLTS scan with a normal majority-carrier trap-filling pulse, Fig. 1 curve (a): it is only observed with the optical pulse. All defects with normal electrical structures that have an electrical level in the upper half of the band gap should be observed in a DLTS experiment employing a majority-carrier electrical trap-filling pulse. As indicated in the preceding section, this anomalous property of the new level is a characteristic signature[22] of a defect with negative-U properties.

The new peak, as observed with an optical trap-filling pulse, disappears upon annealing in a 1:1 correspondence with the disappearance of the E(0.37) interstitial boron peak, as monitored with an electrical trap-filling pulse. Annealing can be either thermal at $\sim$240 K or with minority-carrier injection at temperatures at least as low as 78 K.[12] Correlation is also observed with the growth

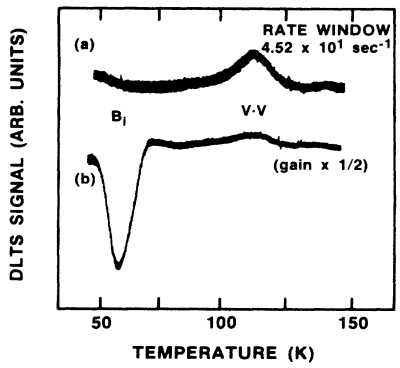

FIG. 2. Typical DLTS runs in p-type silicon after electron irradiation and 175 K anneal with (a) an electrical trap-filling pulse and (b) an optical trap-filling pulse. Again, the B_i peak is visible only when using an optical trap-filling pulse.

of the $E(0.23)$ level that appears when the $E(0.37)$ level disappears.[12,15] [The $E(0.23)$ peak can be observed with either optical or electrical trap-filling pulses.] This correlated behavior upon annealing establishes that the new peak and the $E(0.37)$ level are related to each other.

The new peak can also be observed in p-type silicon with the same optical trap-filling pulses. This is shown in Fig. 2, where the data were taken after annealing to ~ 175 K to remove the interfering vacancy signal [$H(0.13)$].[15,23] In a normal (electrical pulse) DLTS scan, Fig. 2 curve (a), only a single peak is observed which arises from the $H(0.20)$ level of the divacancy.[15,21] When the optical trap-filling pulse is substituted for the electrical pulse, the new peak is seen at ~ 58 K. In Fig. 2 curve (b), the peak appears as a downward-going DLTS signal, indicating that the level is emitting a minority carrier. Since the material is p-type, this means that the signal arises from an electron trap with an energy level in the upper half of the forbidden gap. In p-type material, the new peak disappears upon annealing (under similar conditions as in n-type material) in a 1:1 correspondence with the appearance of the $E(0.23)$ peak. [The $E(0.23)$ peak can be observed with either an optical trap-filling pulse or a forward bias injection trap-filling pulse in the p-type samples.]

An alternative way of studying this new peak in n-type silicon is to modify the normal DLTS experiment in order to avoid the accumulation of centers in the negative charge state. This has been accomplished by continuously illuminating the sample with $0.3\ \text{eV} \lesssim h\nu \lesssim 1.1$ eV light to photoionize those centers in the negative charge state

$$B_i^- \underset{h\nu}{\rightarrow} B_i^0 + e^- \ . \tag{4}$$

The result of this illumination is shown in Fig. 3. With no light present, Fig. 3 curve (a), the A center and the $E(0.09)$ level are detected. When the photoionizing light is turned on, Fig. 3 curve (b), the new peak is observed in the DLTS spectrum.

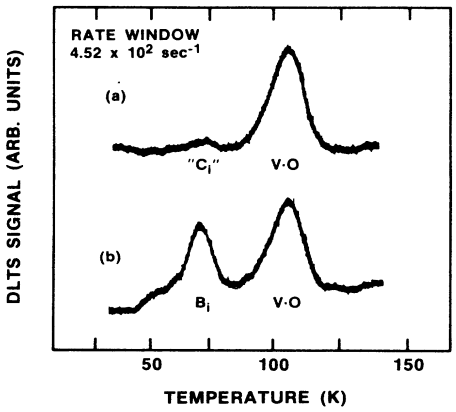

FIG. 3. DLTS spectra in n-type silicon taken with (a) no light present and (b) photoionizing light present. The B_i peak is visible only when the light is present.

The result of a preliminary study of the emission rate of this new level in n-type silicon is shown in (a) of Fig. 4. The data shown in this figure were taken in the presence of photoionizing light with typical electrical trap-filling pulses. Similar results are obtained for the emission rate when an optical-filling pulse is used, in either n-type or p-type silicon. For reference, the emission rate measured for the $E(0.37)$ level is also shown, (b) of Fig. 4. A more detailed study of the emission rate of this new level will be discussed in detail later in this paper, where it will be shown that the emission rate observed by DLTS is enhanced by the electric fields present in the DLTS diode.

B. EPR results

A detailed study of the decay of the photogenerated Si-G28 spectrum was undertaken [Eq. (1)]. The spectrum was photogenerated with near-band-gap light *in situ* at pumped nitrogen temperatures and the rate of its decay monitored. The results are shown in (c) of Fig. 4. The observed decay is given by

$$\tau_{\text{EPR}}^{-1} = (6.8\times 10^{10}) \times \exp[-(0.14\pm 0.01\ \text{eV})]/k_B T]\ \text{sec}^{-1} \ . \tag{5}$$

Assuming that this reflects electron emission from the neutral state, as in Eq. (1), and correcting for the T^2 dependence of the conduction-band thermal velocity and density of states, we obtain an estimate of the donor position as $E_c - (0.13\pm 0.01)$ eV. This study was performed following the initial irradiation of 6.3×10^{16} electrons/cm^2, and checked following the total irradiation of 1.3×10^{17} electrons/cm^2. The same decay rate was obtained in each case indicating that there is a sufficient quantity of other traps present to prevent retrapping of

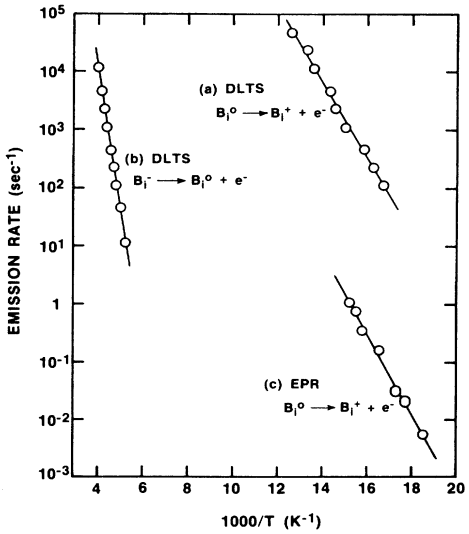

FIG. 4. (a) DLTS emission rate from the $E_c - 0.13$ eV level observed in the presence of photoionizing light. (b) DLTS emission rate from the $E_c - 0.37$ eV level. (c) Decay rate for the metastable B_i^0 EPR spectrum.

the emitted carriers at the emitting interstitial boron atoms. We conclude therefore, that if this interpretation of the decay is correct, Eq. (5) provides a direct measure of the electron emission rate from B_i^0. The discrepancy between the EPR and DLTS results, apparent in Fig. 4, will be resolved later in this paper, where it will be demonstrated that both experiments are indeed monitoring electron emission from the same center. As such, we will refer to both the EPR and DLTS level as the $E(0.13)$ level throughout the rest of this paper.

V. DISCUSSION AND FURTHER RESULTS

A. Negative-U ordering

In order to explore the features of the $E(0.37)$ and the $E(0.13)$ levels, in the presence of photoionizing light, and their relationship to the negative-U model, it is necessary to first optimize several experimental parameters. A schematic representation of the entire capacitance transient after a single trap-filling pulse, in the presence of photoionizing light, is depicted in Fig. 5. Assuming that all of the centers are in the positive charge state before the first trap-filling pulse, the pulse will produce a combination of neutral and negative charge states. The shallower neutral centers can ionize rapidly with time constant τ^0, due to thermal excitation. The deeper negative centers will not thermally ionize at the low temperatures necessary to observe τ^0, but will photoionize with time constant τ_p^-.

The photoionization rate can be adjusted by changing the light intensity. This rate was generally set to be ~ 2 orders of magnitude slower than the thermal emission rate from B_i^0 that was being monitored. This keeps the light level low enough that the thermal ionization of B_i^0 is much faster than any possible photoionization of B_i^0. It also keeps the photoinduced capacitance transient due to the ionization of B_i^- from interfering with the observation of the thermal transient from B_i^0.

By adjusting the time between trap-filling pulses so it is long with respect to τ_p^-, it is guaranteed that all the centers will return to the positive charge state before the next trap-filling pulse. In this way the accumulation of centers in the negative charge state is avoided.

After each pulse, some of the centers are in the neutral charge state and some are in the negative charge state.

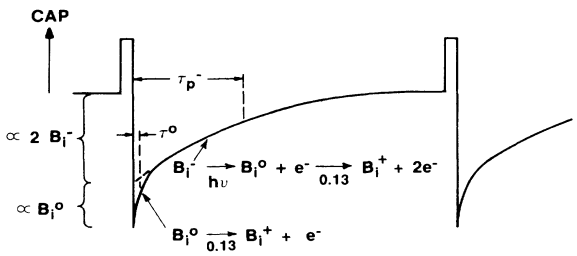

FIG. 5. Schematic representation of the capacitance transient that results from interstitial boron in the presence of photoionizing light.

The component of the capacitance transient due to the ionization of each of these can be monitored separately by appropriately adjusting the DLTS rate window. In Fig. 5, the amplitude of the component of the transient due to the photoionization of B_i^- is indicated as being proportional to twice the concentration of B_i^-. This is because it is a two-electron ionization process that is controlled by the slower photoinduced stage,

$$B_i^- \xrightarrow[h\nu]{} B_i^0 + e^- \xrightarrow[0.13\ \text{eV}]{} B_i^+ + 2e^- \ . \tag{6}$$

The ionization of B_i^0 is straightforward to monitor since it is a thermal transient and therefore a normal DLTS signal will be observed. The photoinduced transient from B_i^- is temperature independent and therefore a normal DLTS signal does not occur. In order to observe this phototransient, the boxcar-rate window must be matched to the photoionization rate. This is most easily done, in practice, by selecting a boxcar-rate window and then varying the light level until the photoionization rate matches the chosen rate window.

Figure 6 shows the recorded DLTS output signal for a fixed-rate window (45.2 sec^{-1}) and several different light intensities (obtained by inserting different transmission screens into the light path). The total ionization rate from the $E(0.37)$ level is the sum of the photoionization rate and the thermal rate

$$\tau^{-1} = \tau_{\text{photo}}^{-1} + \tau_{\text{thermal}}^{-1} \ . \tag{7}$$

With the light off, there is no phototransient and a normal DLTS transient is observed at $T \sim 200$ K [Fig. 6 curve (a)].

When the light is turned on, and the intensity is set so that the phototransient matches the DLTS rate window, the signal shown in Fig. 6 curve (c) is observed. At low

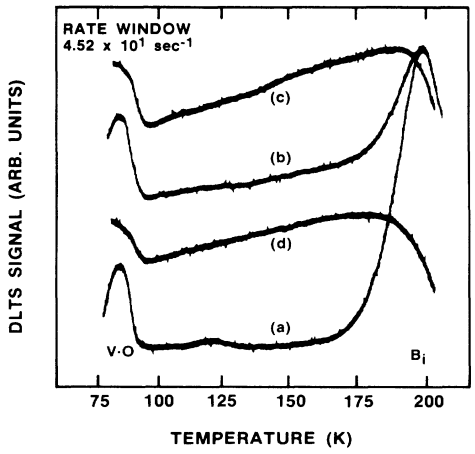

FIG. 6. DLTS signals arising from the $E(0.37)$ level of B_i in the presence of photoionizing light, all recorded with the same fixed-rate window, with (a) no light; (c) the proper amount of light so that the phototransient matches the DLTS rate window; (b) too little light to match the rate window; and (d) too much light to match the rate window.

temperatures, the transient is dominated by the photoinduced rate. Since this rate is temperature independent, a constant signal is recorded until the temperature is high enough that the thermal rate begins to dominate. When this happens, the total rate is now too fast to be matched to the DLTS rate window and the recorded signal decreases. [The variation in amplitude observed in Fig. 6 curve (c) is due to a temperature dependence in the trapping process, not in the emission process. For a trap-filling pulse longer than the one used in this figure, 0.2 μsec, the amplitude is constant until the thermal emission rate begins to dominate.] The peak observed at $\sim$85 K is due to the A center which is present and can also be photoinduced. The dominant contribution to the recorded signal between $\sim$90 K and $\sim$200 K is due to interstitial boron. [There is a small underlying contribution from phosphorus-vacancy pairs at E(0.43) (Refs. 15 and 24–26) which can be subtracted after annealing to remove the B_i signal.]

The DLTS spectra in Fig. 6 curves (b) and (d) show what is observed when the photoinduced transient is not matched to the DLTS rate window. If the light level is set too low, Fig. 6 curve (b), then at low temperatures the phototransient is too slow to match the rate window and a reduced signal is recorded. At higher temperatures, the thermal process begins to contribute and a peak appears as the total rate approaches, matches, and finally exceeds the DLTS rate window. If the light level is set too high, Fig. 6 curve (d), the transient rate is too fast to match the DLTS rate window at all temperatures, and a reduced signal is recorded throughout the scan.

When the light is set properly, the amplitudes of both components of the transient can be determined. It is quite easy to switch DLTS rate windows in the middle of a temperature sweep, so both can be determined during the same scan. This was done in Fig. 7 to obtain the amplitude of both the thermal transient from B_i^0 (rate window $=1.13\times10^4$ sec^{-1}) and the phototransient from B_i^- (rate window $=1.13\times10^2$ sec^{-1}). The baseline for the phototransient was determined after annealing to remove interstitial boron from the sample, as shown in the figure.

The concentration of B_i^0 is proportional to the amplitude of the E(0.13) signal. As there is a temperature dependence to the capture cross section of the negative charge state (apparent in that the signal from the phototransient is not constant versus temperature), it is necessary to extrapolate the phototransient signal down to the temperature at which the E(0.13) peak appears. In this way, both amplitudes are determined under the same conditions. (This extrapolation is also necessary for the baseline run made after interstitial boron was annealed from the sample.) This procedure is illustrated in Fig. 7. The extrapolation to lower temperatures, rather than just recording at the lower temperature, is necessary to avoid including the contribution from unrelated shallower levels. [The low-temperature contribution of the A center is seen clearly in Fig. 6 curve (c). The contribution of the E(0.23) peak that appears when interstitial boron disappears is also avoided in this procedure.] The amplitude of the phototransient in Fig. 7 is indicated as being proportional to twice the concentration of B_i^- because of the two-electron emission involved in this ionization process, Eq. (6).

Using this procedure, it is therefore possible to determine the concentration of both B_i^0 and B_i^- for different trap-filling pulse conditions. This has been done and the results are plotted in Fig. 8. As the trap-filling pulse width is increased, the amplitude of the the E(0.13) peak decreases. This is another anomalous result for a normal level, but again, it is a characteristic signature[22] of a defect with negative-U properties. The longer pulse allows more time for the second electron capture to take place, producing more B_i^-, and thus leaving fewer defects in the one-electron B_i^0 state. The complimentary 1:1 behavior between the two transient decays and the constancy of their sum provide a direct and unambiguous demonstration that these two levels, with inverted emission activation energies, belong to the same defect.

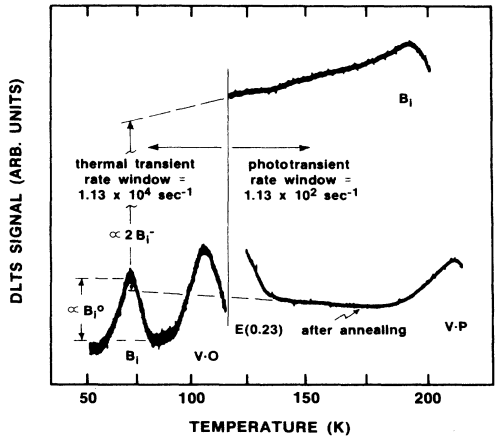

FIG. 7. DLTS runs showing both the thermal decay of B_i^0 and the photoinduced decay of B_i^-. Also indicated is the method for extracting the relative concentrations of each component.

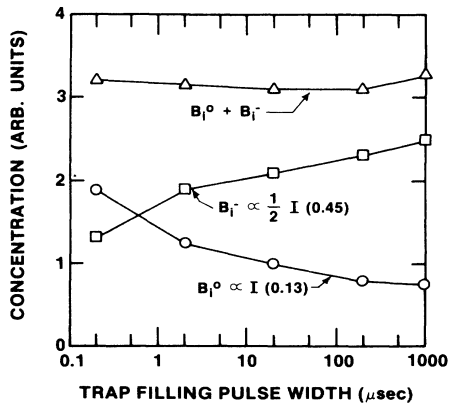

FIG. 8. Concentration of B_i^- and B_i^0 at the end of each trap-filling pulse as deduced from the amplitudes (I) of the corresponding DLTS transients.

B. Electrical level positions

The results of a preliminary DLTS study of the emission rate of the new level have already been discussed in Sec. IV A and are shown in (a) of Fig. 4. These data were taken in the presence of photoionizing light on a p^+n diode with typical electrical trap-filling pulses. Also shown, (c) of Fig. 4, is the rate determined from the EPR decay, Eq. (5). If both of these rates are monitoring the same process, then the two rates should agree. However, there is an unacceptable factor of $\sim 10^3$ difference in the value of the emission rates, as determined by the two techniques.

We find that this discrepancy results from an enhancement of the emission rate by the electric field in the depletion region of the DLTS diode. This is the Poole-Frenkel effect,[27] where the barrier for carrier emission from a Coulombic attractive center is lowered by an amount

$$\Delta E = e\left[\frac{e}{\pi\epsilon\epsilon_0}\right]^{1/2}\mathcal{E}^{1/2}=\beta\mathcal{E}^{1/2}\ , \tag{8}$$

where $\mathcal{E}$ is the electric field, e is the electronic charge, ϵ is the dielectric constant of the material, and ϵ_0 is the permittivity of free space. The analysis of Frenkel predicts for the emission rate[27]

$$\ln e_n(\mathcal{E},T)=\ln e_n(0,T)+(\beta/k_BT)\mathcal{E}^{1/2}\ . \tag{9}$$

To study this, DLTS experiments were performed on the p-type Schottky-barrier diodes using an optical trap-filling pulse. The optical pulse generates the neutral charge state in the entire depletion region of the diode. For a diode with uniform acceptor concentration, the electric field in this region varies linearly from zero at the edge of the depletion region to a maximum value at the junction of

$$\mathcal{E}_{\max}=2\left[\frac{eN}{2\epsilon\epsilon_0}\right]^{1/2}(V+V_B)^{1/2}\ . \tag{10}$$

where V is the applied reverse bias, V_B the built-in junction voltage, and N is the free-carrier concentration in the bulk material. (From *in situ* C^{-2} versus V measurements during the course of the DLTS experiments, we determine the net acceptor concentration to be $N=7\times10^{14}$ cm^{-3} and uniform, with $V_B=0.6$ eV.) The value of $\mathcal{E}_{\max}$ therefore can be as large as $\sim 10^4$ to 10^5 V/cm depending on the applied reverse bias. Consequently, electron emission takes place in the presence of a large range of electric fields which results in a large range of enhancements due to the Poole-Frenkel effect.

In order to have a well-defined electric field, the pulse sequence shown in the inset of Fig. 9 was used. During the optical pulse (i), a small reverse bias V_1 was applied in order to allow only levels near the junction to be filled. After the pulse (ii), a larger reverse bias V_2 was applied. In this way the emitting levels are confined to a narrow range of electric fields, the average of which is given by

$$\mathcal{E}_{\rm av}=\left[\frac{eN}{2\epsilon\epsilon_0}\right]^{1/2}[2(V_2+V_B)^{1/2}-(V_1+V_B)^{1/2}]\ , \tag{11}$$

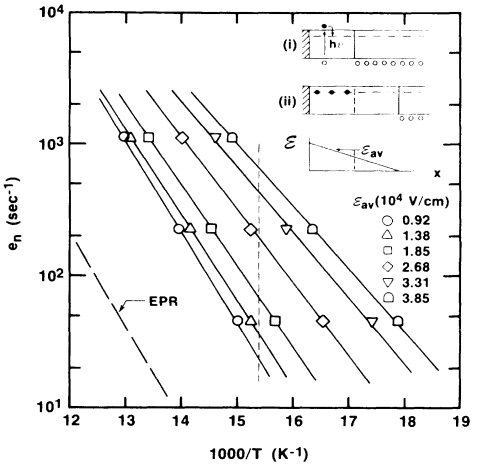

FIG. 9. Temperature dependence of the electron emission rate determined by DLTS for the $E(0.13)$ level vs average electric field in the junction. The EPR result for electron emission from neutral interstitial boron (zero electric field) is also indicated. The inset shows the bias conditions used to obtain a well-defined electric field in the diode junction during emission. The dashed line lies at 65 K, and indicates the interpolated emission rates plotted in Fig. 10.

which can be varied by changing the applied reverse biases, V_1 and V_2. This represents an easy way of obtaining a well-defined electric field for the emitting levels.

Representative emission rates observed at various average electric fields are shown in Fig. 9 as e_n versus $1000/T$. In this figure we note that both the absolute value of the emission rate changes as well as the apparent activation energy (over the range from 0.12 to 0.08 eV), as predicted by Eqs. (8) and (9). In order to fit this data to the Poole-Frenkel model it is desirable to have the emission rate plotted versus electric field at a single temperature. To do this, we have taken the emission rates from Fig. 9 at 65 K, as shown by the dashed line, and replotted the data as e_n versus $\mathcal{E}^{1/2}$ in Fig. 10. (Similar results are obtained at 60 and 70 K, therefore covering the entire region over which the original data in Fig. 9 was taken.)

The solid straight line in Fig. 10, representing the $\mathcal{E}^{1/2}$ dependence predicted by Eq. (9), extrapolates within accuracy of the measured points to the EPR value, also shown. This explains the discrepancy of Fig. 4, and unambiguously confirms that the level observed in the DLTS experiments arise from interstitial boron. In addition, the quantitatively demonstrated Poole-Frenkel effect confirms the single-donor $(0/+)$ character of the $E(0.13)$ level, consistent with the EPR observation of *neutral* B_i^0 when occupied by an electron.

It should be noted that the slope of the solid straight line in Fig. 9 gives a value of β that is $\sim 15\%$ smaller than that predicted by Eq. (8). A best fit to Frenkel's model, Eq. (9), is shown in the figure. However, we do not necessarily expect exact agreement with this equation. In particular, others[28–30] have derived somewhat different forms by extending Frenkel's derivation from one to three

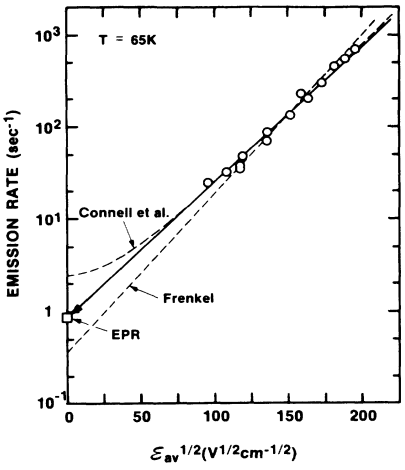

FIG. 10. Dependence of the electron emission rate from neutral interstitial boron on the electric field in the junction at 65 K.

dimensions. For comparison, the prediction of Connell, Camphausen, and Paul[30] is also shown in Fig. 10. The data are not sufficient to judge the merits of either model (it is not possible to rule out a $\sim 10-15\,\%$ error in our estimate of $\mathcal{E}$), but it is interesting that they straddle the EPR result.[31]

In order to derive an electrical level position from emission-rate studies such as these, it is necessary to apply a correction for an emission-capture barrier if it exists. In the case of the $E(0.13)$ level, the existence of a well-behaved Poole-Frenkel effect rules out the possibility that such a barrier exists. (The $\mathcal{E}^{1/2}$ dependence confirms the smooth $1/\epsilon r$ attractive Coulomb potential.) We conclude therefore that the single-donor level of interstitial boron is at $E_c-(0.13\pm0.01)$ eV, and no correction is necessary.

The case of the deeper acceptor level must be separately considered. In the previous studies,[12] the capture cross section was too large to be measured directly ($\gtrsim 10^{-16}$ cm^2) with no evidence of a temperature dependence. It was tentatively concluded therefore that the barrier correction was small. In our present experiments, however, with very short filling pulses (0.2 μsec), and a much wider range of temperature available, a weak temperature dependence has been observed, as noted in Figs. 6 curve (c) and 7. From these figures, the capture time constant at 100 K can now be estimated to be $\tau\sim 0.15$ μsec, which leads to an estimate of the capture cross section at that temperature of

$$\sigma=\frac{1}{\langle v_{th}\rangle n\tau}\sim 3\times10^{-17}\ \text{cm}^2\ ,$$

where $n\sim 2\times10^{16}$ cm^{-3} and $\langle v_{th}\rangle\sim 10^7$ cm/sec. We note that this is a factor of ~ 100 less than the characteristic geometrical cross section $\sigma_\infty\sim 3.5\times10^{-15}$ cm^2 expected and often observed for the extrapolated $T\rightarrow\infty$ value in semiconductors.[32] This suggests that a barrier may indeed exist. We may make a rough estimate of its magnitude as follows.

As pointed out by Lang,[33] the cross section for multiphonon carrier capture should have the form

$$\sigma=\sigma_\infty\exp(-E_b/k_BT^*)\ , \tag{12}$$

where

$$k_BT^*=\frac{\hbar\omega}{2}\coth\left[\frac{\hbar\omega}{2k_BT}\right]\ . \tag{13}$$

Here E_b is the capture barrier and ω is an average phonon frequency associated with the dominant defect relaxation mode and the resulting capture barrier. (For $\hbar\omega/2k_BT>1$, k_BT^* approaches $\hbar\omega/2$, reflecting temperature-independent capture by tunneling through the barrier.)

The results of Fig. 6 curve (c) indicate a gradual increase in the cross section by a factor of ~ 2 over the range 100–175 K. With Eqs. (12) and (13), this matches a characteristic phonon energy of ~ 35 meV, a reasonable value [representing an average between TO (~ 60 meV) and TA (~ 15 meV) phonons]. With this, and $\sigma_\infty\sim 3.5\times10^{-15}$ cm^2, we obtain a barrier height of ~ 0.083 eV. According to this, the acceptor level should be given therefore by

$$\sim E_c-0.45+0.08=E_c-0.37\ \text{eV}\ .$$

This is, of course, only an approximate estimate. To determine this more accurately, it would be necessary to have available a sample with substantially lower net donor concentration so that precise cross-section measurements could be made.

We can put an upper limit to the barrier by assuming $\omega=\omega_{TO}=62$ meV, the highest phonon available. With this, the barrier height becomes ~ 150 meV and the level is located at $E_c-0.30$ eV. (This value of ω predicts a temperature-independent cross section from 100–175 K, inconsistent with the results of Figs. 6 and 7, and therefore clearly provides an overestimate of E_b.)

In view of these uncertainties, we estimate the level position for the acceptor level to be

$$E(-/0)=E_c-(0.37\pm0.08)\ \text{eV}\ , \tag{14}$$

where the error estimate fully brackets the range of possibilities.

VI. MODEL

The negative-U properties of interstitial boron have therefore been firmly established, the single-acceptor level at $E_c-(0.37\pm0.08)$ eV lying inverted below the single donor level at $E_c-(0.13\pm0.01)$ eV as summarized in Fig. 11. The net effective correlation energy U is $-(0.24\pm0.09)$ eV, a surprisingly large negative value. Normally $U\sim+0.2-0.3$ eV for deep levels in silicon.[34,35] We can conclude therefore that a relaxation energy of ~ 0.5 eV is involved in going from $B_i^0\rightarrow B_i^-$, implying a substantial lattice rearrangement.

The EPR results[10] have established firmly that B_i^0 is in a low-symmetry (C_{1h}) position, which can be characterized by a small distortion in a $\{110\}$ plane away from a position of axial $\langle 111\rangle$ symmetry (C_{3v}). It was further

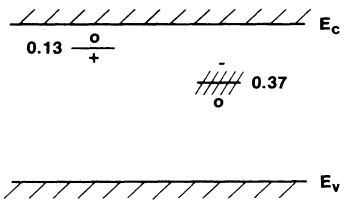

FIG. 11. Electrical level structure for interstitial boron in silicon, showing the negative-U ordering in the donor and acceptor levels.

found in these studies that, in the $B_i^0 \rightleftarrows B_i^+$ conversion, the ⟨111⟩ axis of the defect is unchanged but the memory of the off-axis distortion is lost. From this it was suggested that B_i^+ is in a pure ⟨111⟩ axial configuration and in the conversion to B_i^0 it "puckers" out into one of the six possible off-axis directions provided by the three {110} planes containing this axis. The barrier for thermally activated reorientation from one ⟨111⟩ axis to another is substantial, having been measured to be 0.6 eV. It was found, however, that optical excitation with near-band-gap light is capable of causing ⟨111⟩ defect axis reorientation. From this it was postulated that in the B_i^- state, produced by optical excitation, the boron atom changes its configuration substantially, providing access to other ⟨111⟩ distortion directions as it converts back to the neutral charge state by capturing a hole.

Two microscopic models that have been suggested[10,12] are reproduced in Figs. 12 and 13. In Fig. 12, the ion flips from a bond-centered position for B_i^+ to a split-⟨100⟩ configuration for B_i^-. In Fig. 13, the defect moves between the hexagonal interstitial site for B_i^+ to the B_i^- split-⟨100⟩ configuration. A third suggested model[10] replaces the $(Si\text{-}B\text{-}Si)^{0,+}$ arrangement of Fig. 12 with $(Si\text{-}Si\text{-}B)^{0,+}$, the configuration for B_i^- still being possibly that of a split-⟨100⟩ dumbbell. All of these can be considered consistent with the EPR results for the intermediate B_i^0 state.

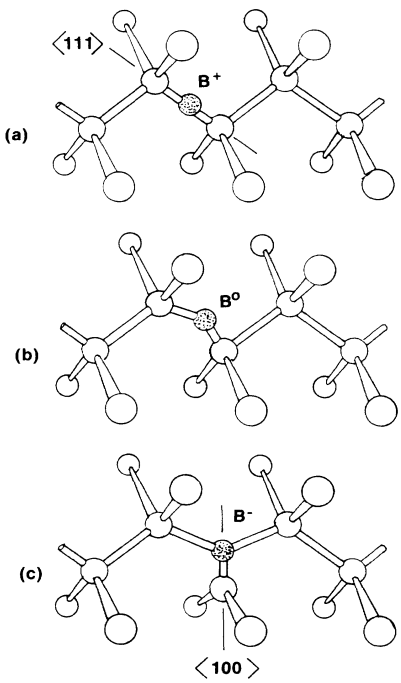

FIG. 12. Suggested model for the lattice configurations of interstitial boron vs charge state (Refs. 10 and 12).

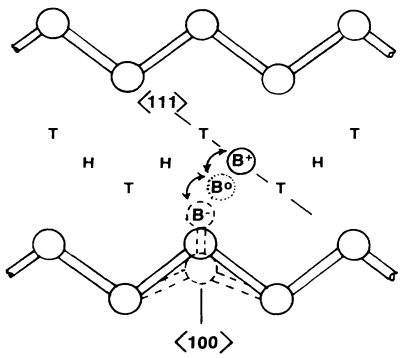

FIG. 13. Alternative model for the interstitial boron configurations (Refs. 10 and 12). Shown are the lattice atoms and the normal tetrahedral (T) and hexagonal (H) sites in a {110} plane.

Our present results shed no new light to help distinguish between these microscopic models. Our results do provide important confirmation, however, that a substantial lattice rearrangement must take place between B_i^0 and B_i^-, consistent with the rebonding arrangements suggested for B_i^-. The estimate that we have made for the lattice-relaxation energy of ~ 0.5 eV is strongly suggestive of rebonding.

Further evidence of large lattice relaxation is in the observation of recombination-enhanced migration of the defect.[12] In these studies it was found that the migration rate is proportional to the square of the injected minority-carrier current in either p- or n-type material which was interpreted to indicate that the complete cycle $B_i^+ \rightleftarrows B_i^0 \rightleftarrows B_i^-$ is required for a lattice jump. This is fully consistent with the models of Figs. 12 and 13 for which the B_i^- configuration forms a "saddle point" for B_i^+ migration and vice versa. Such motion is called the "Bourgoin-Corbett" mechanism.[36] Recent experiments[37] have shown, however, that it cannot be quite that simple. Simply cycling between charge states by capture and emission of electrons does not appear to cause motion. Apparently the energy released upon hole capture is essential. This implies either that one or the other of the two charge extremes is not a true saddle position or that additional barriers exist.

There remain, therefore, many intriguing questions about the microscopic configurations and processes. Some of these questions may be answered by further EPR experiments which are currently under consideration. But another important approach is theory. Modern quantum-mechanical computational techniques have proven very successful recently in calculating total energies of

defect configurations in semiconductors.[38–42] In our view there is no more challenging a problem than that of interstitial boron in silicon about which we now know so much. We strongly encourage theorists to tackle this important model system.

In any case, the observed dangling-bond character of the EPR B_i^0 state and the changes in bonding configurations indicated by the large lattice-relaxation energy and the proposed models suggest that this system should be considered a close analogue to the valence-alternation pair models proposed by Kastner *et al.*[5]

VII. SUMMARY

Photo-DLTS experiments have been employed to detect a new electrical level of interstitial boron located at $E_c-(0.13\pm0.01)$ eV. By comparison of its emission rate with that determined by EPR experiments, through the Poole-Frenkel effect, it has been conclusively shown that this level arises from interstitial boron. The quantitatively demonstrated Poole-Frenkel effect confirms that the $E(0.13)$ level is the single donor $(0/+)$ level. The 1:1 correspondence between the trap-filling pulse-width dependence of the $E(0.13)$ level and the previously detected $E(0.37)$ level demonstrates that they belong to the same defect, the deeper level being the single-acceptor level $(-/0)$ and emitting two electrons. Correcting for a capture barrier, the acceptor level is determined to be at $E_c-(0.37\pm0.08)$ eV. These results combine to demonstrate conclusively that interstitial boron in crystalline silicon has negative-U properties.

ACKNOWLEDGMENTS

Helpful discussions are gratefully acknowledged with L. C. Kimerling, who first suggested the Poole-Frenkel effect to us, and L. A. Ledebo, who suggested the pulsing sequence for its study. This research was supported by the U.S. Navy Office of Naval Research Electronics and Solid State Science Program under Contract No. N00014-76-C-1097.

---

*Present address: Standard Oil Research & Development, 4440 Warrensville Center Rd., Cleveland, Ohio 44128.

†Present address: Solarex Corporation, Thin Film Division, 826 Newtown-Yardley Rd., Newtown, PA 18940.

[1]For a recent review of negative-U properties in solids, see G. D. Watkins, in *Festkörperprobleme* Vol. XXIV of Advances in Solid State Physics, edited by P. Grosse (Vieweg, Braunschweig, 1984), p. 163.

[2]J. Hubbard, Proc. R. Soc. London, Ser. A **276**, 238 (1963).

[3]P. W. Anderson, Phys. Rev. Lett. **34**, 953 (1975).

[4]R. A. Street and N. F. Mott, Phys. Rev. Lett. **35**, 1293 (1975).

[5]M. Kastner, D. Alder, and H. Fritzche, Phys. Rev. Lett. **37**, 1504 (1976).

[6]R. D. Harris, J. L. Newton, and G. D. Watkins, Phys. Rev. Lett. **48**, 1271 (1982).

[7]J. L. Newton, A. P. Chatterjee, R. D. Harris, and G. D. Watkins, Physica **116B**, 219 (1983).

[8]M. Stavola, M. Levinson, J. L. Benton, and L. C. Kimerling, in *Thirteenth International Conference on Defects in Semiconductors,* edited by L. C. Kimerling and J. M. Parsey, Jr. (AIME, Warrendale, PA, 1985), p. 191.

[9]Z. Vardeny and J. Tauc, Phys. Rev. Lett. **54**, 1844 (1985).

[10]G. D. Watkins, Phys. Rev. B **12**, 5824 (1975).

[11]G. D. Watkins and J. R. Troxell, Phys. Rev. Lett. **44**, 593 (1980).

[12]J. R. Troxell and G. D. Watkins, Phys. Rev. B **22**, 921 (1980).

[13]In Refs. 11 and 12, the level position was estimated to be $E_c-(0.45\pm0.02)$ eV. Corrections for a capture-emission barrier, to be presented in Sec. V B of the present paper, provide a new estimate of $E_c-(0.37\pm0.08)$ eV. To avoid confusion, we will refer to it throughout the paper as the $E(0.37)$ level.

[14]D. V. Lang, J. Appl. Phys. **45**, 3014 (1974); **45**, 3023 (1974).

[15]J. R. Troxell, Ph.D. thesis, Lehigh University, 1979 (unpublished).

[16]G. D. Watkins and J. W. Corbett, Phys. Rev. **121**, 1001 (1961).

[17]G. D. Watkins and J. W. Corbett, Phys. Rev. **134**, A1359 (1964).

[18]L. C. Kimerling, P. Blood, and W. M. Gibson, in *Defects and Radiation Effects in Semiconductors—1978,* Proceedings of the Conference on Defects and Radiation Effects in Semiconductors, Inst. Phys. Conf. Ser. No. 46, edited by J. H. Albany (IOP, London, 1979), p. 273.

[19]R. D. Harris and G. D. Watkins, in *Thirteenth International Conference on Defects in Semiconductors,* edited by L. C. Kimerling and J. M. Parsey, Jr. (AIME, Warrendale, PA, 1985), p. 799.

[20]Recent studies [L. W. Song, B. W. Benson, and G. D. Watkins, Phys. Rev. B **33**, 1452 (1986)] have challenged this identification, suggesting that the defect may be vacancy related.

[21]L. C. Kimerling, in *Radiation Effects in Semiconductors—1976,* Proceedings of the Conference on Radiation Effects in Semiconductors, Inst. Phys. Conf. Ser. No. 31, edited by N. B. Urli and J. W. Corbett (IOP, London, 1977), p. 221.

[22]As pointed out in Ref. 8, it is not *proof,* however. If the capture-emission barriers are large enough, it is possible to have inverted emission activation energies without negative-U. This question will be addressed in Sec. V B.

[23]G. D. Watkins, in *Lattice Defects in Semiconductors—1974,* Proceedings of the Conference on Lattice Defects in Semiconductors, Inst. Phys. Conf. Ser. No. 23, edited by F. A. Huntley (IOP, London, 1975), p. 1.

[24]L. C. Kimerling, H. M. DeAngelis, and C. P. Carnes, Phys. Rev. B **3**, 427 (1971).

[25]M. Hirata, M. Hirata, and H. Saito, J. Phys. Soc. Jpn. **27**, 405 (1969).

[26]A. O. Evwaraye, Appl. Phys. Lett. **29**, 476 (1976).

[27]J. Frenkel, Tech, Phys. USSR **5**, 685 (1938); Phys. Rev. **54**, 647 (1938).

[28]A. K. Jonscher, Thin Solid Films **1**, 213 (1967).

[29]J. L. Hartke, J. Appl. Phys. **39**, 4871 (1968).

[30]G. A. N. Connell, D. L. Camphausen, and W. Paul, Philos. Mag. **26**, 541 (1972).

[31]It has been pointed out [W. Keller, G. Pense, and M. Schulz, Physica **116B**, 244 (1983)] that random electric fields due to charged defects in the junction may also alter significantly the electric field dependence of the effect. Our linear dependence on $\mathcal{E}^{1/2}$ shows little of the radical departure predicted by these workers but residual efects may still be operative.

[32]C. H. Henry and D. V. Lang, Phys. Rev. B **15**, 989 (1977).

[33]D. V. Lang, in *Fifteenth Internationl Conference on Semiconductors, Kyoto, 1980* [J. Phys. Soc. Jpn., Suppl. A, **49**, 215 (1980)].

[34]G. G. DeLeo, G. D. Watkins, and W. B. Fowler, Phys. Rev. B **25**, 4972 (1982).

[35]A. Zunger and U. Lindefelt, Phys. Rev. B **26**, 5989 (1982).

[36]J. C. Bourgoin and J. W. Corbett, Phys. Lett. **38A**, 135 (1972).

[37]R. D. Harris, G. D. Watkins, and L. C. Kimerling, in *Fourteenth International Conference on Defects in Semiconductors,* edited by H. J. von Bardeleben [Mater. Sci. Forum, **10-12**, 163 (1986)]. See also *Note added in proof* in Ref. 12.

[38]G. G. DeLeo, W. B. Fowler, and G. D. Watkins, Phys. Rev. B **29**, 3193 (1984).

[39]R. Car, P. J. Kelly, A. Oshiyama, and S. T. Pantelides, Phys. Rev. Lett. **52**, 1814 (1984).

[40]Y. Bar-Yam and J. D. Joannopoulos, Phys. Rev. Lett. **52**, 1129 (1984).

[41]G. A. Baraff and M. Schluter, Phys. Rev. B **30**, 3460 (1984).

[42]M. Scheffler, E. Beeler, O. Jepsen, O. Gunnarsson, O. K. Andersen, and G. B. Bachelet, in *Thirteenth International Conference on Defects in Semiconductors,* edited by L. C. Kimerling and J. M. Parsey, Jr. (AIME, Warrendale, PA, 1985), p. 45.